ORIGINAL ARTICLE

A microalgal biorefinery approach for bioactive molecules, biofuel, and biofertilizer using a novel carbon dioxide-tolerant strain *Tetradesmus obliquus* CT02

Ankan Sinha[1] · Gargi Goswami[2] · Ratan Kumar[1] · Debasish Das[1]

Abstract
A microalgal biorefinery approach has been established through bioprospecting of an indigenous CO_2-tolerant freshwater isolate *Tetradesmus obliquus* CT02 biomass in two sequential steps, resulting in alternate product cascades of bioactive molecules and biodiesel or biofertilizer. In the first step, crude microalgal extracts in five different solvents were screened for their antioxidant and anticancer activities. While acetone extract showed the highest antioxidant activity with an IC_{50} value of 137 µg mL^{-1}, ethyl acetate extract exhibited maximum anticancer activity with an IC_{50} value of 306.67 µg mL^{-1}. This antioxidant and anticancer activity may be attributed to the coordinated action of multiple bioactive molecules as detected by HR-LCMS analysis. In the next step, post extracted residual biomass of CT02 was evaluated as feedstock for biodiesel production. The lipid content was found to be 35.7–39.1% w/w, and further to that, FAME yield of 33.1–36.7% w/w was obtained via direct transesterification of both the acetone and ethyl acetate extracted biomass. Analysis of FAME composition revealed an abundance of palmitic acid (C16:0), stearic acid (C18:0), and elaidic acid (C18:1n9t) as the major constituents, making it suitable for use as biodiesel. The post extracted residual biomass was also evaluated for its application as biofertilizer through induced germination of *Solanum lycopersicum* seeds. The highest final germination percentage and germination index was estimated to be in the range of 75–80% and 117.5–118.5, respectively, comparable to that of commercial grade NPK (20:20:13).

Keywords Microalgal biorefinery · CO_2-tolerant strain · Antioxidant · Anticancer · Biodiesel · Biofertilizer

1 Introduction

The alarming deterioration in air quality due to CO_2 emission from various anthropogenic activities has mandated the search for natural resources, such as microalgae, facilitating carbon capture and its biological conversion into value-added products. Microalgae, photoautotrophic eukaryotes with the ability to produce high-value compounds and bulk chemicals, can exhibit enhanced growth rate and biomass productivity compared to terrestrial plants [1]. However,

selection of robust and indigenous microalgal strains with potential of sequestering CO_2 and subsequent conversion into multiple value-added products, in a biorefinery mode, is the key to the development of sustainable bioprocess.

Though microalgae have been well documented as feedstock for biofuels, the technology is not completely mature to be realized at the commercial scale owing to low net energy ratio (NER) and sub-optimal economic output. One of the potential solutions to these bottlenecks could be a biorefinery approach which enables sequential valorization of the microalgal biomass towards co-production of high-value metabolites (biotherapeutics, nutraceuticals, and pigments), biofuels (biodiesel, bio-crude oil, and bioethanol), and other low-value products (biofertilizer and bioplastics). In contrast to the process with single product strategy, biorefinery with multiple products may offer a sustainable and efficient process via maximizing the economic, environmental, and social benefits. For instance, a biorefinery strategy was demonstrated for generation of *Scenedesmus* sp. [2]

✉ Debasish Das
debasishd@iitg.ac.in; debasish.iitg@gmail.com

1 Department of Biosciences & Bioengineering, Indian Institute of Technology Guwahati, Guwahati, Assam 781039, India

2 Department of Biotechnology, Gandhi Institute of Technology and Management (GITAM) University, Visakhapatnam, Andhra Pradesh 530045, India

utilizing waste water and subsequent conversion of biomass into a wide range of high-value products such as phenols or flavonoids and low-value products such as biofuel or biofertilizer. In another study [3], *Nannochloropsis* sp. was used as a platform to produce carotenoids and biodiesel, while the residual biomass was utilized as substrate for dark fermentation to produce biohydrogen. Techno-economic analysis [4] has shown that, in spite of having a vast global market, commercial availability of microalgal products is still in dormancy due to high capital cost and operational cost. To that end, the integrated approach of biofuel production coupled with bioprospecting of value-added products has been found to offer process sustainability and economic viability.

In the present study, a biorefinery approach has been established with an indigenous CO_2-tolerant freshwater microalgal isolate towards synthesis of bioactive molecules, biofuel, and biofertilizer. Screening and isolation of this CO_2-tolerant strain was performed by a novel CO_2 selection pressure-based screening strategy. The isolate was evaluated in terms of growth under different physicochemical parameters and biochemical composition, thereby obtaining insight about prospective product options. The concept of biorefinery with multiple products has been demonstrated in two sequential steps resulting in alternate product cascades: option 1 being bioactive molecules and biodiesel or option 2 being bioactive molecules and biofertilizer. In the first step, solvent-based crude microalgal extracts containing bioactive molecules were screened for their antioxidant and anticancer activities. Crude fractions exhibiting antioxidant and anticancer activities were further characterized through mass spectroscopy to identify the bioactive molecules. The post extracted biomass was subjected to a two-step direct transesterification method for biodiesel production as another product of option 1. In case of option 2, the post extracted biomass obtained from the first step was evaluated for its biofertilizer potential through induced germination of *Solanum lycopersicum* seeds.

2 Materials and methods

2.1 Sampling, screening, and isolation of potential CO_2-tolerant microalgal strain

As a CO_2-rich industrial hotspot, sample was collected from effluent of Bokaro Steel Plant, Jharkhand, India (23.6693° N, 86.1511° E) and was inoculated in BG11 medium [5] in a bubble column reactor (Spectrochem Instruments Pvt. Ltd., India) of 500 mL with working volume of 300 mL and enriched to obtain sufficiently large cell population. Screening of CO_2-tolerant strains was performed by a novel CO_2 selection pressure-based screening strategy, where the enriched mixed culture was exposed to sequentially elevated

concentrations of CO_2 starting from 5 to 20% v/v, with stepwise increase by 2.5% v/v. The CO_2 concentration of the input gas stream was varied by ratiometric mixing of compressed air and CO_2 through rotameters. The culture was maintained at room temperature with a light–dark cycle of 16:8 h and light intensity of approximately 250 $\mu E\ m^{-2}\ s^{-1}$. In order to eliminate any possible nutritional stress, the concentrations of nitrate and phosphate were maintained higher than 50% of their initial value via intermittent feeding. Dynamic profiles of phosphate and nitrate utilization and pH were obtained by sampling every 24 h at the end of the light cycle. The screened CO_2-tolerant culture, at the end of the batch of 53 days, was subjected to serial dilution and streak plating to isolate axenic unialgal culture.

2.2 Identification of the isolated strain

The morphology of the strain was studied using bright field microscopy (Nikon, Japan) and field emission scanning electron microscopy (FESEM) (Sigma, Carl Zeiss Microscopy, Germany). For molecular identification of the strain, genomic DNA was isolated using HiPurA™ plant genomic DNA purification kit, and partial 28 s rDNA sequence was amplified using D2 region specific primers (forward being ACCCGCTGAACTTAAGC and reverse being GGTCCGTGTTTCAAGACGG) in a thermal cycler (Veriti®, Thermo Fisher Scientific, USA). PCR amplification conditions involved an initial denaturation step at 94 °C for 5 min, followed by 35 cycles of 94 °C for 1 min, 52 °C for 1 min, and 72 °C for 2 min and final extension of 10 min at 72 °C. Further, sequencing of the PCR amplicon was performed using BDT v3.1 Cycle sequencing kit on ABI 3730xl Genetic Analyzer. The sequence obtained was compared with the existing database through NCBI BLAST, and the phylogenetic tree was constructed in MEGA X using Neighbor-Joining method with 1000 bootstrap replications.

2.3 Characterization of the strain under different physiochemical parameters in shake flask

Characterization experiments were performed to study the effect of different medium composition, initial pH of the medium, nitrogen, and phosphate sources on growth of the organism. In order to understand the suitable medium supporting maximum biomass titer, growth characterization was carried out in five different medium compositions such as Watanabe (AF6), Beijerinck (BJA), BG 11, Bold Basal medium (BBM), and Algae Culture Broth (ACB). Details about the composition of these media are given in Supporting Information (Table S1). Further, the growth of the strain was evaluated under various initial pH (4, 6, 8, 10, and 12),

different nitrogen sources (sodium nitrate, sodium nitrite, ammonium sulfate, analytical grade urea, and commercial grade urea) with equimolar nitrogen (0.011 M), and different phosphate sources (monopotassium phosphate, dipotassium phosphate, and single super phosphate) containing equimolar phosphate (0.0015 M). All characterization experiments were performed in 250 mL Erlenmeyer flasks with working volume of 100 mL, incubated at 28 °C temperature and 150 rpm agitation in a shaker incubator (Orbitek, Scigenics Biotech, India). 10%, v/v of seed culture with absorbance (A_{690}) of 1.0 was used as inoculum, and the light intensity was maintained at 20 µE m^{-2} s^{-1} with a light/dark cycle of 16:8. Samples were withdrawn at the end of every light cycle to monitor the growth. After completion of growth characterization, the biochemical composition of the biomass and CO_2 fixation rate was evaluated under selected physiochemical parameters supporting improved growth.

Biomass productivity (P, mg L^{-1} day^{-1}) and CO_2 fixation rate (R_{CO_2}, mg L^{-1} day^{-1}) was calculated as follows:

$$P = \frac{x_f - x_0}{t_f - t_0} \tag{1}$$

where x_0 and x_f are the dry cell weights (g L^{-1}) obtained at initial and final time points t_0 and t_f, respectively.

$$R_{CO_2} = C_C P \frac{M_{CO_2}}{M_C} \tag{2}$$

where C_C is elemental carbon content of biomass. M_{CO_2} and M_C are the molar mass of CO_2 and C (g mol^{-1}), respectively. C_C was estimated at the end of the batch using elemental analyzer (EuroEA3000, Italy).

2.4 Preparation of microalgal crude extracts

One gram finely powered lyophilized biomass was suspended in 50 mL of each of the five solvents, i.e., methanol, isopropanol, acetone, ethyl acetate, and hexane. These solvents were chosen based on their difference in polarity. Five different crude extracts were prepared by three rounds of sonication and overnight incubation at 28 °C and 150 rpm, followed by evaporation of the solvent (Fig. S1, Supporting Information). The crude extracts were stored at 4 °C for subsequent experiments.

2.5 Determination of antioxidant activity through DPPH free radical scavenging

The antioxidant activity of the crude extracts was determined in terms of 2,2-diphenyl-1-picrylhydrazyl (DPPH) radical scavenging activity assay [6]. The concentration of each extract required to scavenge 50% of the DPPH (IC_{50}) was calculated based on the correlation (linear regression) between percentage scavenging activity and concentration of the extract. In order to develop the correlation, different concentrations (50–1000 µg mL^{-1}) of each crude extract were prepared in methanol. The crude extract in methanol (0.75 mL) was mixed with 0.25 mL of 0.1 mM DPPH, dissolved in methanol, and incubated for 30 min in dark at room temperature. Post incubation, the absorbance of the mixture was recorded at 517 nm. DPPH scavenging activity (%) was calculated as follows:

$$\% \, DPPH \, scavenging \, activity = \frac{A_c - A_t}{A_c} \times 100 \tag{3}$$

where A_c is the absorbance of control containing DPPH dissolved in pure methanol and A_t is the absorbance of the test sample together with DPPH.

2.6 Screening and estimation of anticancer activity of the crude extracts

The effect of microalgal crude extract on cancer cell growth inhibition was determined in vitro through MTT-based cell viability assay [7]. In the first step, all five extracts were evaluated for their anticancer activity at a concentration of 100 µg mL^{-1}. Breast cancer cells (MCF7) grown in DMEM high glucose medium were seeded in 96 well plate (4000–5000 cells per well). After 48 h of incubation at 37 °C and 5% v/v CO_2, the monolayer was washed with DPBS. Prior to MTT assay, the cells were treated with the extract or with ethanol (vehicle control) for 72 h. Base line viability was determined by performing the MTT assay for the cells at zero h. Post treatment, monolayer of the cells was washed with DPBS and incubated with 100 µL MTT reagent (0.5 mg mL^{-1}) for 3 h at 37 °C. MTT reagent was then removed, and the formazan crystals were dissolved in DMSO. Absorbance was measured at 570 nm using microplate reader (Infinite Pro M200, Tecan Life Sciences, Switzerland), with 690 nm as the reference. The difference in the absorbance (A_{570}—A_{690}) was considered as the measure for cell viability. Change in viability of ethanol-treated cells (control) was assigned as 100%, and those of extract treated cells were expressed as relative to the control. The extract exhibiting highest inhibition to the cell viability was selected for further experiments. The IC_{50} for the selected extract was calculated based on the percentage cell viability observed at different concentrations.

2.7 Identification of compounds with antioxidant and anticancer activity using HR-LCMS-QTOF

Phytochemical composition of the selected crude microalgal extracts exhibiting maximum antioxidant and anticancer activities was analyzed by high-resolution liquid chromatograph

mass spectrometer (HR-LCMS, 1290 Infinity UHPLC System, Agilent Technologies, USA). The system was aided with Quadrupole Time of Flight Mass Spectrometer (Q-TOF MS). Five-microliter sample was injected into the Hypersil Gold C18 column (100×2.1 mm – 3 μ particle size). Gradient of water with 0.1% formic acid (solvent A) and acetonitrile with 10% water and 0.1% formic acid (solvent B) was used as mobile phase. With a flow rate of 3 mL min^{-1}, separation was performed for 30 min. Compounds were analyzed in 6550 iFunnel Q-TOF MS operated in positive ion mode by dual Agilent jet stream electrospray ionization (dual AJS ESI). Mass spectrometric data acquisition was done for the m/z ratio ranging 150 to 1000 with a scanning rate of 1 spectrum per second. Metlin Metabolites AM PCD Library (B.08.00) (Agilent Technologies, USA) was used for identification of compounds. The compounds found in abundance were further reviewed for their antioxidant and anticancer activities based on previously reported literatures.

2.8 Assessment of post extracted residual microalgal biomass as feedstock for biodiesel production

The FAME content of the post extracted residual microalgal biomass was estimated using sequential two-step direct transesterification method [5]. In the first step, 1 mL alkali catalyst (0.5 N NaOH in methanol) was added to 50 mg of dry biomass followed by incubation at 90 ℃ in a shaker water bath at 150 rpm for 20 min. After cooling down, the second step was performed by adding 1 mL acid catalyst (5% H_2SO_4 in methanol) and incubating at the same conditions. Finally, the FAME fraction was collected by adding equal volume of deionized water and hexane to the transesterified mixture. Hexane layer containing total FAME was washed thrice in order to remove aqueous impurities. The FAME components were analyzed using GC-FID (Agilent Technologies, USA). FAME dissolved in hexane was filtered through 0.22 μ nylon filter and injected to GC equipped with HP-5 ms Ultra Inert column (30 m × 250 μm × 0.25 μm). Helium was used as carrier gas, and the split ratio was set as 10:1. Oven temperature was ramped from 70 to 180 ℃ at a rate of 15 ℃ min^{-1} and then to 260 ℃ at rate of 2.5 ℃ min^{-1}, and the final temperature was held for 5 min. The total runtime for GC-FID analysis was 44.33 min. Supelco 37 component FAME mix (Sigma-Aldrich, USA) was used as the standard for identification and quantification of compounds.

2.9 Assessment of post extracted residual microalgal biomass as biofertilizer

The potential of post extracted residual microalgal biomass as biofertilizer was assessed based on its effect on the germination of *Solanum lycopersicum* (tomato) seeds. In petri plates, 100 gm of air-dried soil (sieved through 2-mm mesh) was mixed with different amounts (11.5 mg, 50 mg, 75 mg, 100 mg, 125 mg, 150 mg, 175 mg, and 200 mg) of residual microalgal biomass or commercial grade NPK (20:20:13) to obtain the different fertilizer doses. Each plate was inoculated with 10 tomato seeds and kept in greenhouse at 25 ℃ temperature and 70% humidity. Fixed amount of tap water was sprinkled on each plate at every 24-h interval. All the plates were monitored for number of seeds germinated every 24 h. At the end of the 10th day, the final germination percentage (FGP) and the germination index (GI) were calculated according to Eq. 4 and Eq. 5, respectively [2].

$$FGP = \left(\frac{\text{Total no. of seeds germinated at the end of trial}}{\text{number of initial seeds}} \right) \times 100 \quad (4)$$

$$GI = (10 \times N_1) + (9 \times N_2) + (8 \times N_3) + (7 \times N_4) + (6 \times N_5) \\ + (5 \times N_6) + (4 \times N_7) + (3 \times N_8) + (2 \times N_9) + (1 \times N_{10}) \quad (5)$$

where N_t is the number of seeds germinated on the tth day and value of t varies from 1 to 10.

Further to this, NPK content of the residual microalgal biomass was measured to quantitatively establish its biofertilizer capacity. Total nitrogen (N) was determined directly by elemental analyzer (EuroEA3000, Italy). Total phosphorus (P) was determined following the procedure described by Feng et al. [8] and estimated calorimetrically using ascorbic acid method [9]. For estimation of potassium (K), 10 mL of mixed acid reagent (H_2SO_4:HCLO$_4$::5:1) was added to 0.2 g of biomass and digested at 300 ℃ for 4 h [10]. Quantification of potassium (K) was done using flame photometry.

2.10 Analysis of growth, substrate utilization, and intracellular biochemical composition

For monitoring the growth of the organism, absorbance of the culture was measured at 690 nm (A_{690}) using UV–Vis spectrophotometer (Cary 100, Agilent Technologies, USA). The absorbance values were converted into dry cell weight (DCW) using the correlation, one cell density = 0.1853 g dry cells L^{-1} ($R^2 = 0.99$). Cell-free supernatant obtained from centrifugation of the sample at 10,000 rpm for 10 min was analyzed for substrate utilization. Estimation of nitrate was carried out using salicylic acid method using sodium nitrate as the standard [11], and phosphate was quantified using ascorbic acid method [9] using dipotassium phosphate as the standard. For biochemical composition analysis, stationary phase culture was collected and centrifuged at 7000 rpm at 4 ℃ for 10 min. Cell pellet was washed twice with distilled water and lyophilized overnight. To extract the intracellular protein, biomass resuspended in phosphate buffer (pH 6.8)

was subjected to ultrasonication at 35% amplitude (a maximal power of 350 W) in a pulse mode (5 s ON/10 s OFF) under cold condition. Repeating 3 rounds of sonication for 5 min each, the supernatant was collected after every round. Total protein estimation of the whole supernatant was carried out by Bradford method [12] using bovine serum albumin as standard. 0.25 mL of protein sample extracted was mixed with 2.5 mL of Bradford reagent, and absorbance was recorded at wavelength of 595 nm. For extraction of intracellular chlorophyll, 50 mg of dry biomass was resuspended in 10 mL of 99.9% methanol and incubated in dark at 45 ℃ for 30 min. The sample was then centrifuged, and supernatant was analyzed for absorbance at wavelength of 652 nm and 665 nm. Total chlorophyll content (sum of chlorophyll a and chlorophyll b) was estimated based on Eq. 6 and Eq. 7 [13].

$$Chlorophyll\ a\left(\mu g\ mL^{-1}\right) = 16.5169 \times A_{665} - 8.0962 \times A_{652} \tag{6}$$

$$Chlorophyll\ b\left(\mu g\ mL^{-1}\right) = 27.4405 \times A_{652} - 12.1688 \times A_{665} \tag{7}$$

The intracellular lipid was estimated by thermo-gravimetric analysis [14]. Two milliliters of methanol/chloroform (2:1) was mixed with 50 mg of dry biomass and sonicated for 30 min (35% amplitude, 5 s ON/10 s OFF) at 4 ℃. The mixture was then incubated for 6 h with shaking at 150 rpm in room temperature. Further, the lipid was extracted with chloroform layer by repeated washing with chloroform:0.9% NaCl (1:2). The extracted lipid was weighed and compared to the initial biomass for valuation of total intracellular lipid. Total carbohydrate content was estimated via phenol sulfuric acid method [15], using glucose as standard. Prior to the assay, dried microalgal biomass was subjected to acid hydrolysis by incubation with 4% sulfuric acid at 121 ℃ for 1 h. Ash content of the biomass was calculated by subjecting 1 gm of dry biomass to 575 ℃ in a muffle furnace for 4 h.

3 Results and discussion

3.1 Screening and isolation of CO_2-tolerant microalgal strain from industrial hotspot

Under photoautotrophic condition, microalgae grow by fixing CO_2 from different sources such as the atmosphere and exhausts from industries including flue and flare gas. The growth rate of microalgae is directly proportional to the photosynthetic efficiency which in turn depends on the available CO_2 concentration. It has been reported that atmospheric concentration of CO_2 (0.036%) is sub-optimal for photosynthesis [16], and the photosynthesis apparatus appears to be adapted to much higher concentrations of CO_2 [17]. Further, microalgal bioprocess is typically based on flue gas from

various industries, CO_2 concentration in which varies from 3 to 30% [16]. Therefore, screening and isolation of an indigenous CO_2-tolerant strain remains the first key step towards development of a sustainable bioprocess. In the present study, a CO_2 selection pressure-based strategy was adopted for rapid screening and isolation of CO_2-tolerant microalgal strain. The water sample collected from carbon-rich industrial hotspot was subjected to culturing under sequentially elevated CO_2 concentration of 5–20% v/v, with a step-wise increase by 2.5%. In the beginning of the screening process, starting with 5% CO_2 v/v, presence of four morphologically distinct microalgal strains was accounted in the mixed culture, and their growth was monitored in terms of differential cell count. A consistent lag in the growth of the strains was observed at the beginning of each elevation of CO_2 selection pressure. With the increase in CO_2 concentration, reduction in growth of the strains was observed, and finally, three out of four strains could survive under the final CO_2 concentration of 20% v/v. Amongst the three survivors, only one strain was found to not only withstand but also grow significantly even at 20% CO_2 concentration v/v and was further isolated. The growth of the strain could be correlated with the decrease in concentration of nitrate and phosphate during the batch run under individual concentration of CO_2. pH of the culture was found to be automatically maintained within the range of 7–8 even at higher CO_2 concentrations. This self-regulatory phenotypic response might be due to continuous utilization of CO_2 linked with growth of the organism, even at higher CO_2 selection pressure [18]. In a similar study, microalgal community present in the waste water sample collected from sewage treatment plant was enriched at high CO_2 concentration of 10% v/v, and *Scenedesmus* sp. was found to grow dominantly amongst all microalgal strains present in the mixed culture [19].

3.2 Identification and characterization of the isolated microalgal strain

Bright field microscopy and FESEM images (Fig. 1 a and b) confirmed the oval-shaped unicellular nature of the isolated microalgal strain and absence of any spike or flagella on the cell surface. The cells were visibly green in color and about 6 to 9 μm in length. Molecular identification of the isolate was further carried out by 28 s rDNA sequencing analysis as morphological resemblance is only presumptive and do not confirm the evolutionary position of an isolate. The isolate was found to be in closest homology with *Tetradesmus obliquus* KMC24 with maximum sequence similarity of 97.8%. To further depict the evolutionary position of the isolate, a phylogenetic tree was constructed based on the sequence of the isolate and 15 closest organisms (Fig. 1c). In accordance with this finding, the isolated microalgal strain was identified as *Tetradesmus obliquus* CT02 (GenBank

Accession # MZ267545). Hereafter, the organism is designated as CT02.

In search of suitable nutritional and growth conditions for CT02, characterization of the strain was carried out under different media compositions, various initial pH, nitrogen sources, and phosphate sources of the medium supporting maximum growth of CT02. Dynamic profile of growth of CT02 under different nutritional and physicochemical conditions is depicted in Fig. Fig. S2 (Supporting Information). Although the strain was found to grow in a wide variety of culture media (Fig. 2a), the highest biomass titer of 1.087 g L^{-1} was obtained using algae culture broth (ACB) medium. The strain was able to favorably grow at lower initial pH of the medium. A maximum biomass titer of 0.826 g L^{-1} was obtained at a pH value of 6, while sub-optimal growth was observed at alkaline pH (Fig. 2b). Studies depict the initial pH of the medium in the range of 6 to 9 as optimal for the growth of various microalgae [5, 20, 21]. In case of *Scenedesmus* sp., while higher growth was achieved at initial pH close to neutral, synthesis of different growth and non-growth associated products was induced at an acidic pH of 5 [22]. This depicts a mutually exclusive nature of the initial pH conditions promoting growth and product formation. To that end, the present strain may be beneficial as the growth is favorable at lower initial pH of the medium (4–6) which might also promote synthesis of various value-added compounds. Amongst five different nitrogen sources, the strain exhibited a substantially higher biomass titer (0.845 g L^{-1}) with sodium nitrate as compared to others (Fig. 2c). Sodium nitrate has been recognized as a favorable nitrogen source for growth of various microalgal strains [23, 24]. The lower growth in case of ammonia-based nitrogen sources such as ammonium sulfate and urea may be due to the formation of H^+ ions during ammonia uptake from media [5]. Dipotassium phosphate was found to be the most suitable phosphate source for CT02, resulting in highest biomass titer of 0.994 g L^{-1} (Fig. 2d). Under the nutritional conditions of sodium nitrate as nitrogen source, dipotassium phosphate as phosphate source, and initial pH of 6, the maximum biomass productivity and CO_2 fixation rate were found to be 39.7 mg L^{-1} day^{-1} and 66.5 mg L^{-1} day^{-1}, respectively (Table 1). A lower biomass titer of less than 1 g L^{-1} might be a limiting factor for any biorefinery considering the use of CT02. In order to improve the biomass titer and productivity of CT02, different process engineering strategies such as growth kinetic driven feeding of limiting nutrients [25], dynamic increase in incident light intensity [25, 26], and substrate driven pH control [27] can be implemented.

To evaluate the application potential of the biomass with the ability to produce value-added compounds and biofuels, analysis of biochemical composition such as total protein, carbohydrate, lipid, and ash content was carried out (Table 1). A high protein content of 35.96% w/w was estimated, which can be considered potential source of bioactive metabolites [28]. Total chlorophyll content was estimated to be 1.8 µg per mg of biomass. Further, substantially high lipid content of 41.21% w/w depicts that the protein extracted biomass can be suitably used for synthesis of biodiesel. However, carbohydrate content was estimated to be lowest at 11.5% w/w, which may be due to regular consumption of carbohydrate for cellular metabolism as explained by Mirón et al. [29]. Furthermore, the low carbohydrate and high lipid content of biomass at the end of the batch might be the effect of nutritional stress to the cells caused by exhaustion of limiting nutrients nitrate and phosphate, which redirect the carbon flux from carbohydrate or protein fractions of the biomass to the accumulation of neutral lipid [5]. The residual ash content was calculated to be 11.31% w/w.

3.3 Microalgal biorefinery approach for bioactive molecules, biofuel, and biofertilizer using *Tetradesmus obliquus* CT02

Several studies have suggested that the biomass composition can widely vary with difference in microalgae strains, medium composition, culture conditions, and growth phases [30, 31]. High protein and lipid content of CT02 under the given nutritional and growth parameters point towards establishing a circular bioeconomy, coupling CO_2 sequestration, and multiproduct portfolio such as high-value bioactive compounds, biofuel, and biofertilizer, in a biorefinery approach.

3.3.1 Evaluation of crude extracts of CT02 for their antioxidant activity

Antioxidants serve as the crucial defense system against free radicals such as reactive oxygen species (ROS) and reactive nitrogen species (RNS) which causes oxidative stress to the cells leading to their death via oxidation of biological macromolecules [32]. Besides chemically synthesized drugs, several naturally occurring bioactive compounds with antioxidant properties, originating from plants, have been commercially approved [33, 34]. However, increasing market demand owing to population inflammation has motivated the exploration of more cost-effective natural sources like microalgae for these phytochemicals. In the present study, five different solvent-based crude extracts of CT02 were evaluated for their antioxidant potential in terms of DPPH free radical scavenging activity (Fig. 3). All the five crude extracts exhibited dose-dependent antioxidant activity, with the lowest IC_{50} value of 137 µg mL^{-1} in case of acetone extract. While both isopropanol and ethyl acetate extracts showed antioxidant activity (~203 µg mL^{-1}) comparable to that of acetone, hexane extract showed inferior
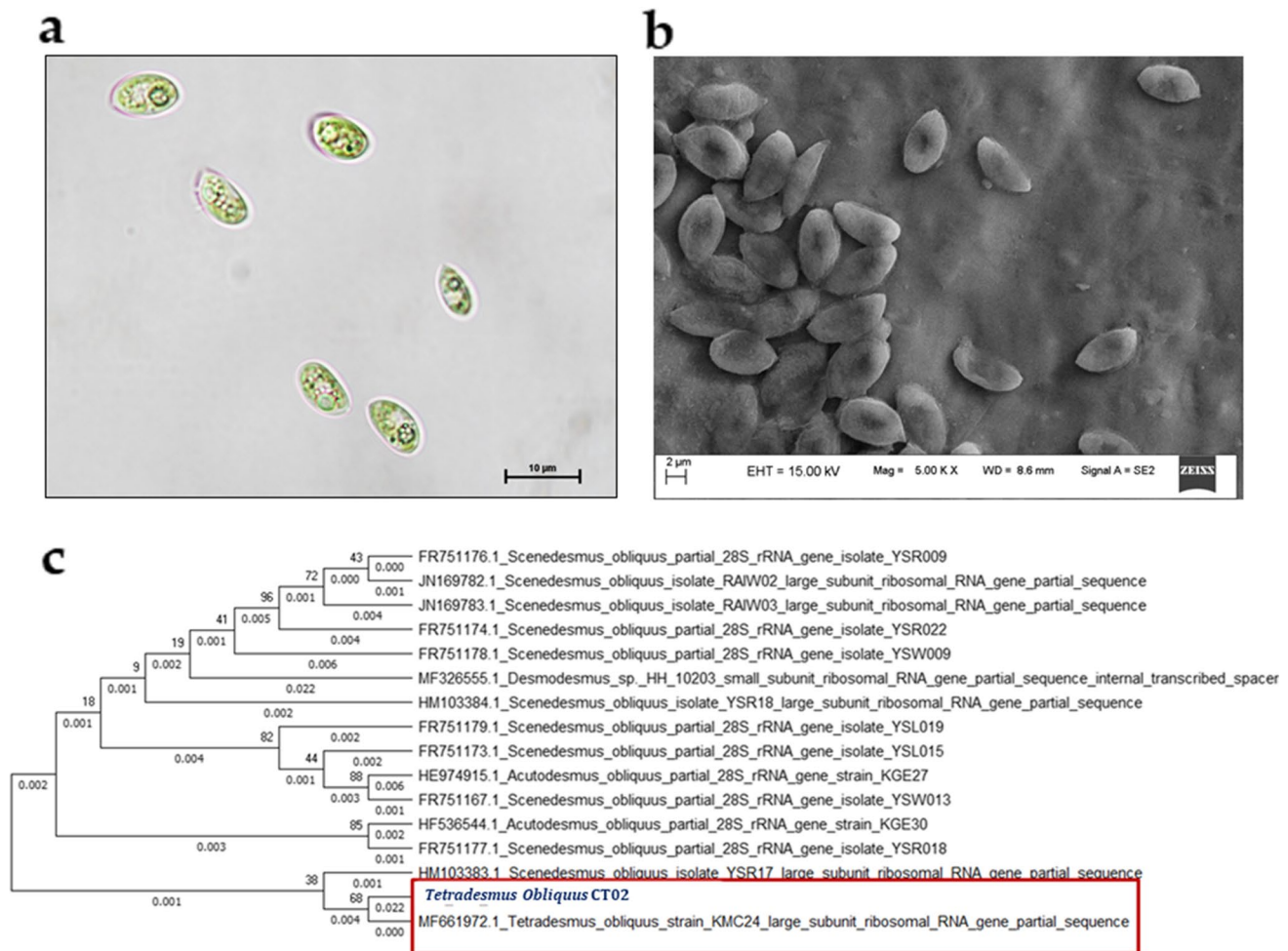
Fig. 1 Morphological identification of isolated microalgal strain under **a** bright field microscopy and **b** field emission scanning electron microscopy (FESEM). The molecular level identification was carried out based on phylogenetic tree generated using MEGA X (**c**). Neighbor-joining showing phylogenetic position of isolate and related taxa is based on partial 28 s rRNA gene sequence comparisons. Bootstrap values are indicated at nodes. Representative sequences in the dendrogram were obtained from GenBank

antioxidant activity with an IC_{50} value of 783.2 µg mL^{-1}. Microalgae have been reported to possess a vast range of bioactive compounds which vary in terms of their polarity and thereby solubility in different solvents. This means that the type and concentration of bioactive molecule(s), obtained post solvent extraction, will vary depending on the polarity of the solvent(s) used for the process of extraction. Hence, differential bioactivity may be observed with different solvent extracts. Acetone extract from CT02 recorded superior antioxidant activity in comparison to other microalgae strains such as *Chlorella* sp. with IC_{50} value of 780–2590 µg mL^{-1} [35], *Scenedesmus obliquus* with IC_{50} value of 938–2273 µg mL^{-1} [36], *Porphyridium sordidum* with IC_{50} value of 286 µg mL^{-1} [37], and *Haematococcus pluvialis* with IC_{50} value of 528 µg mL^{-1} [37]. HR-LCMS-QTOF analysis of acetone crude extract was carried out to identify the compounds with antioxidant property (Table 2). The antioxidant compounds which were found to be present in abundance are fusarochromanone [38], benzoquinol [39], hexadecanoic acid [40], Nigakihemiacetal A [41], luciferin [42], convallasaponin A [43, 44], and tridecanol [46, 47]. Further, brassinolide was reported to enhance the activity of antioxidant enzymes in *Chlorella vulgaris* [45]. Therefore, the antioxidant activity of acetone extract may be attributed to the coordinated action of these bioactive molecules. The results indicate that acetone extracts of CT02 can be commercially realized as potential sources of antioxidant compounds.

3.3.2 Evaluation of crude extracts of CT02 for their anticancer activity

In view of the undesired side effects of conventional chemotherapeutic drugs, the pharmaceutical research is now more

Fig. 2 Growth characterization of *Tetradesmus obliquus* CT02 under **a** different media composition, **b** different initial pH, **c** different nitrogen sources, and **d** different phosphate sources. The duration of the cultivation was considered until the end of logarithmic phase of growth (approximately 23–26 days)
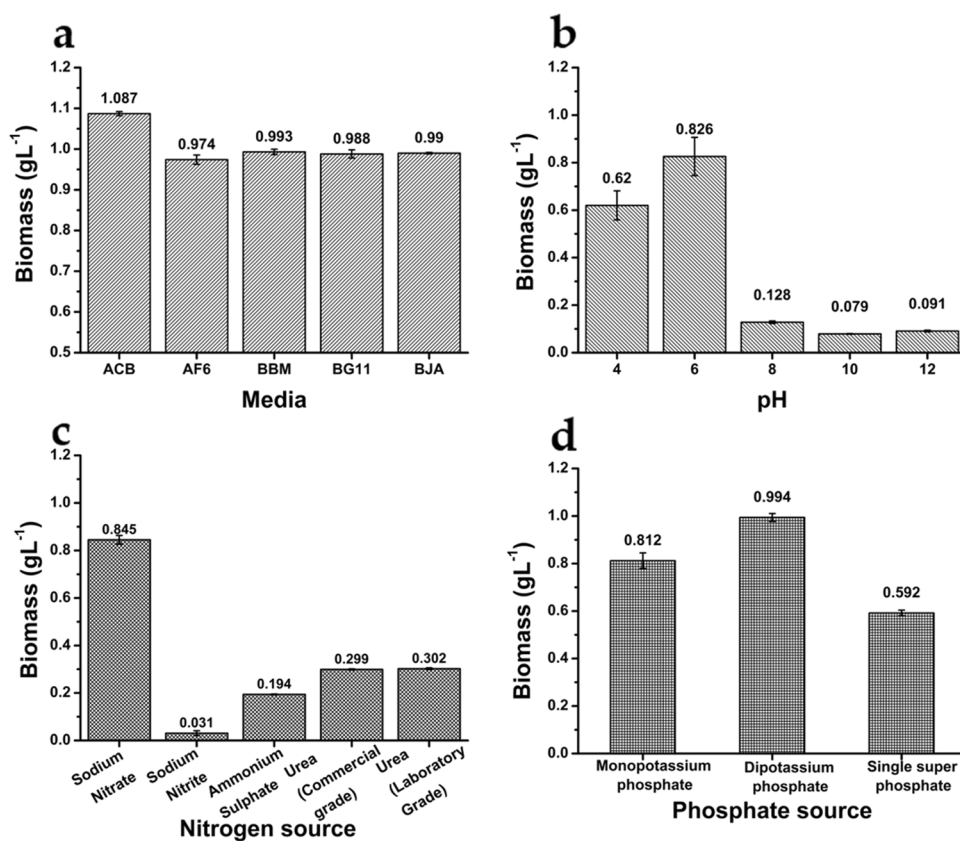

Table 1 Growth kinetic parameters and biochemical composition of *Tetradesmus obliquus* CT02 under selected nutritional and pH condition

Growth kinetic parameters	
Maximum biomass titer (g L^{-1})	0.99 ± 0.02
Biomass productivity (mg L^{-1} day^{-1})	39.7 ± 0.69
CO$_2$ fixation rate (mg L^{-1} day^{-1})	66.5 ± 1.15
Biomass composition	
Carbohydrate (% w/w)	11.52 ± 0.49
Protein (% w/w)	35.96 ± 2.03
Lipid (% w/w)	41.21 ± 1.60
Residual ash (% w/w)	11.31 ± 0.07

focused on search for naturally occurring anticancer agents. Crude solvent extracts obtained from CT02 were screened in vitro for their anticancer activity. At a concentration of 100 μg mL^{-1}, ethyl acetate extract showed the lowest relative cell viability of 73.3%, followed by acetone (77.4%), hexane (83.1%), isopropanol (89.6%), and methanol (91.7%) (Fig. 4a). Further, dose-dependent activity of ethyl acetate extract revealed an IC$_{50}$ value of 306.67 μg mL^{-1} (Fig. 4b). Similar to the present study, anticancer molecules from various microalgae strains such as *Scenedesmus obliquus*, *Chlorella sorokiniana*, and *Granulocystopsis* sp., have shown fairly promising clinical significance against cancer cell

lines [57–59]. HR-LCMS-QTOF analysis of ethyl acetate crude extract revealed the presence of two most prevalent anticancer compounds dioscin [48] and cholanoic acid [49]. Besides, eight more anticancer molecules were also found to be present in abundance (Table 2).
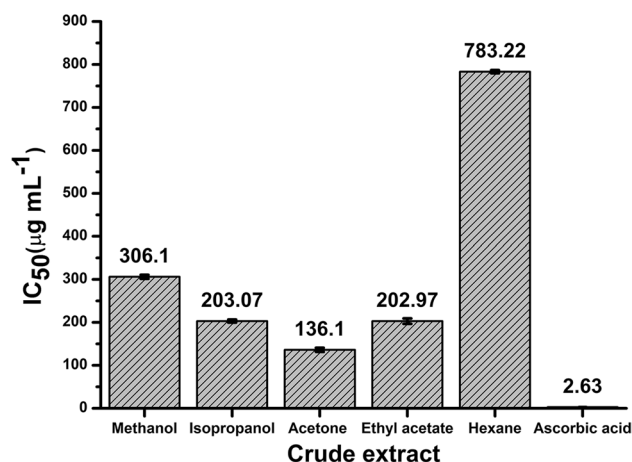

Fig. 3 Comparison of antioxidant activity of different crude extracts of *Tetradesmus obliquus* CT02 based on their IC$_{50}$ for DPPH radical scavenging

Table 2 List of compounds present in selected crude microalgal extracts for antioxidant and anticancer activity identified via HRLCMS-QTOF

Sl. no	Name	Formula	Mass	Relative abundance (%)*	References
Antioxidants present in acetone extract					
1	3′-N-Acetyl-4′-O-(14-methylheptadecanoyl) fusarochromanone	$C_{35}H_{56}N_2O_6$	600.41	6.29	[38]
2	2-Hexaprenyl-3-methyl-5-hydroxy-6-methoxy-1,4-benzoquinol	$C_{38}H_{58}O_4$	578.43	6.16	[39]
3	16-Hydroxy hexadecanoic acid	$C_{16}H_{32}O_3$	272.23	5.97	[40]
4	Nigakihemiacetal A	$C_{22}H_{34}O_7$	410.23	5.71	[41]
5	Dinoflagellate luciferin	$C_{33}H_{40}N_4O_6$	588.30	4.86	[42]
6	Convallasaponin A	$C_{32}H_{52}O_9$	580.37	1.83	[43, 44]
7	Brassinolide	$C_{28}H_{48}O_6$	480.34	1.74	[45]
8	Tridecan-1-ol	$C_{13}H_{28}O$	200.21	1.36	[46, 47]
Anticancer agents present in ethyl acetate extract					
1	Dioscin	$C_{45}H_{72}O_{16}$	868.48	20.09	[48]
2	(5b,12a), 9-anthracenylmethyl ester, 12-hydroxy-Cholan-24-oic acid	$C_{39}H_{50}O_3$	566.39	18.90	[49]
3	Dinoflagellate luciferin	$C_{33}H_{40}N_4O_6$	588.30	4.97	[50]
4	16-Hydroxy hexadecanoic acid	$C_{16}H_{32}O_3$	272.23	3.73	[40]
5	Gracillin	$C_{45}H_{72}O_{17}$	883.49	2.58	[51]
6	Phytosphingosine	$C_{18}H_{39}NO_3$	317.29	2.34	[52]
7	3′-N-Acetyl-4′-O-(14-methylheptadecanoyl) fusarochromanone	$C_{35}H_{56}N_2O_6$	600.41	2.05	[53]
8	Tridecan-1-ol	$C_{13}H_{28}O$	200.21	1.46	[54]
9	Decyl butanoate	$C_{14}H_{28}O_2$	228.21	1.45	[55]
10	TG (18:1(11Z)/16:1(9Z)/18:1(11Z)) [iso3]	$C_{55}H_{100}O_6$	856.75	0.31	[56]

*Relative abundance (%) $= \dfrac{abundance\ of\ a\ molecule\ present\ in\ an\ individual\ extract}{\sum abundance\ of\ all\ the\ molecules\ present\ in\ an\ individual\ extract} \times 100$

3.3.3 Synthesis of biodiesel from post extracted residual biomass of CT02

Analysis of total lipid content of post extracted residual biomass revealed negligible loss with the total lipid content in case of acetone and ethyl acetate, being 39.1% w/w and 35.7% w/w respectively (Table 3). This can be explained by the fact that a major portion of the total microalgal lipid is composed of triacylglycerol, which being non-polar in nature remains unextracted when polar solvents like acetone and/or ethyl acetate are used. The results suggest that both the residual biomass can be used as suitable feedstock for biodiesel production. A total FAME yield of 36.7% w/w

and 33.1% w/w was obtained by direct transesterification of acetone and ethyl extracted biomass, respectively (Table 3). FAME composition has been reported to influence the fuel properties of biodiesel such as cetane number, viscosity, flow properties, and lubricity [60]. FAME obtained from both residual biomasses contained palmitic acid (C16:0), stearic acid (C18:0), and elaidic acid (C18:1n9t) as the major constituents (Fig. 5), thereby making it suitable for use as biodiesel [61, 62]. The absence of C18:3 or other higher unsaturated fatty acids may be advantageous towards better biodiesel quality as per European standards [63]. Further, presence of a high percentage of saturated fatty acids (Table 3) may be beneficial in terms of providing higher

Fig. 4 a Evaluation of crude extracts of *Tetradesmus obliquus* CT02 for their anticancer activity at a concentration of 100 μgmL^{-1} and **b** evaluation of dose-dependent anticancer activity of ethyl acetate extract. Experiments were conducted on breast cancer cell line MCF7
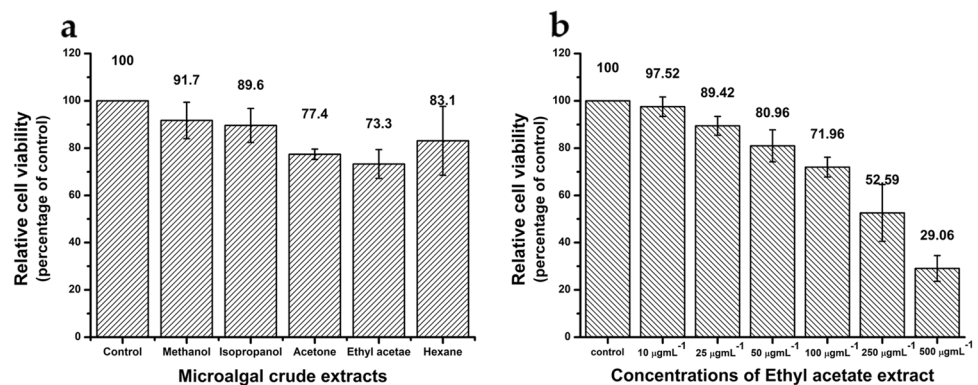
Table 3 FAME profile obtained via direct transesterification of CT02 biomass, before and after extraction

	Dried biomass (before extraction)	Residual biomass (post acetone extraction)	Residual biomass (post ethyl acetate extraction)
Total lipid content (Percentage of biomass)	41.2	39.1	35.7
Total FAME content (Percentage of biomass)	38.6 ± 4.2	36.7 ± 2.4	33.1 ± 1.6
Saturated FAME (Percentage of total FAME) (Percentage of biomass)	59.80 ± 1.19 / 23.09 ± 1.77	61.73 ± 2.5 / 22.65 ± 1.05	69.54 ± 1.1 / 23.02 ± 0.79
PUFA (Percentage of total FAME) (Percentage of biomass)	3.48 ± 0.37 / 1.34 ± 0.10	3.03 ± 0.25 / 1.11 ± .05	5.21 ± 1.2 / 1.72 ± 0.06
MUFA (Percentage of total FAME) (Percentage of biomass)	36.72 ± 2.1 / 14.17 ± 1.09	35.24 ± 2.84 / 12 ± .6	25.25 ± 5.5 / 8.36 ± .29

oxidative stability to biodiesel and improving its performance at low temperature [64].

3.3.4 Application of post extracted residual biomass as biofertilizer

Both the residual biomass, after extraction using acetone and ethyl acetate, has been observed to induce germination of *Solanum lycopersicum* (Tomato) seeds. Compared to control, an increase in final germination percentage (FGP) of 30% and 25% was observed for the residual biomass post acetone and ethyl acetate extraction, respectively (Fig. 6a). The highest FGP of 80% and 75% was observed for acetone

and ethyl extracted biomass at concentrations of 1.25 and 1.5 g per kg soil, respectively (Fig. 6a). These values were found to be comparable with the FGP value of 85% in case NPK (20:20:13), albeit at a lower standard dose of 0.115 g per kg of soil [65]. Based on the daily observation, highest germination index (GI) was recorded to be 118.5 and 117.5 for acetone and ethyl acetate extracted biomass, respectively, both at a concentration of 1.25 g per kg of soil (Fig. 6b). However, a marginally higher GI value of 150 was calculated for NPK (20:20:13) at a dose of 1 g per kg of soil. More than two-fold increase in GI, with respect to control, was observed for both types of residual biomass (Fig. 6b). In a similar study, microalgal pellets of *Scenedesmus*
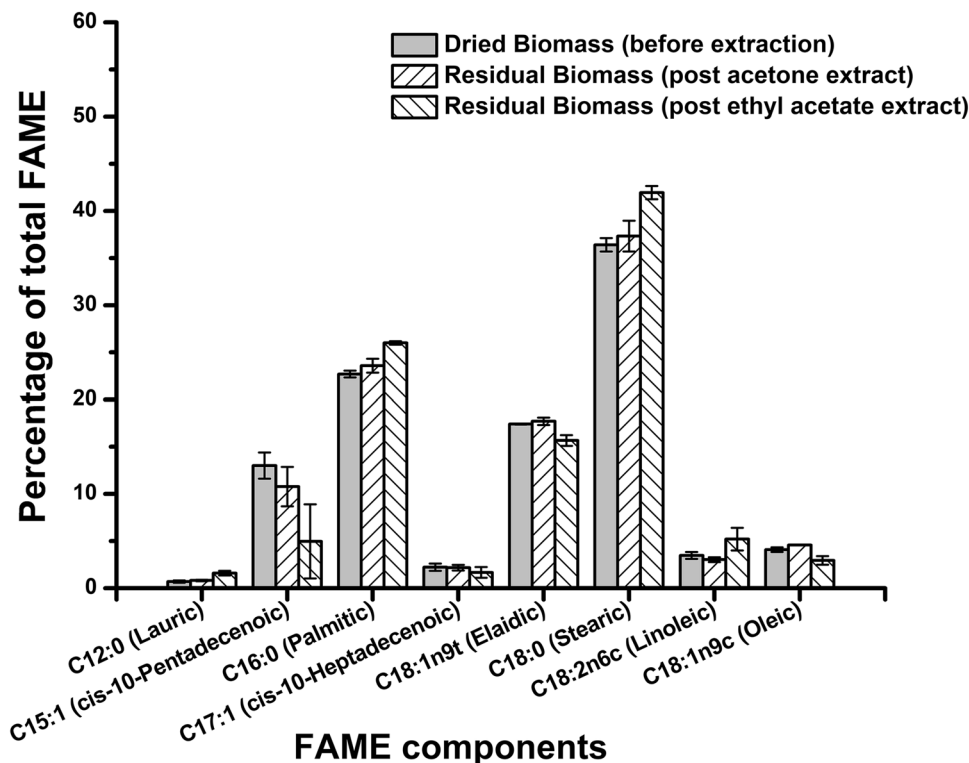

Fig. 5 Composition of FAME obtained via direct transesterification of CT02 biomass before and after extraction

Fig. 6 Dose-dependent effect of post extracted residual biomass of CT02 and NPK on **a** final germination percentage (FGP) and **b** germination index (GI) of *Solanum lycopersicum* (tomato) seeds
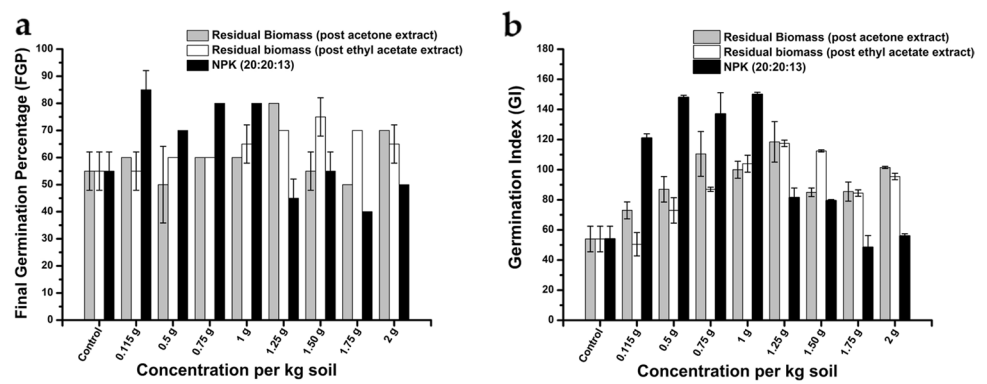

Table 4 Elemental composition (N-P-K) of post extracted biomass of CT02, de-oiled microalgal biomass from *Scenedesmus* sp., and vermicompost

Elements (% of biomass)	Residual biomass post acetone extraction (current study)	Residual biomass post ethyl acetate extraction (current study)	De-oiled microalgal biomass from *Scenedesmus* sp. [66]	Vermicompost [66]
Total N	8.00 ± 0.14	7.30 ± 0.11	7.50 ± 0.08	1.40 ± 0.03
Total P	0.11 ± 0.00	0.12 ± 0.00	1.60 ± 0.03	0.77 ± 0.01
Total K	0.57 ± 0.01	0.50 ± 0.01	0.70 ± 0.02	0.48 ± 0.01

obliquus showed approximately 20% increase in FGP and 1.6-fold increase in GI for germination of wheat and barley seeds [2]. Elemental composition analysis of both the residual biomass revealed presence of 7–8% N, 0.11% P, and 0.5% K (Table 4). This N-P-K composition of the post extracted residual biomass of CT02 was found to be similar to that of de-oiled microalgal biomass (DOMBW) of *Scenedesmus* sp. and vermicompost (Table 4). While the de-oiled biomass of *Scenedesmus* sp. was demonstrated as a promising biofertilizer for rice production [66], vermicompost is considered one of the most commercially used biofertilizers [66]. These results establish the suitability of the post extracted residual biomass of CT02 as biofertilizer.

4 Conclusions

Tetradesmus obliquus CT02, an indigenous microalgal strain isolated through novel CO_2 selection pressure-based screening strategy, found to exhibit a high CO_2 tolerance of up to 20% v/v. Growth of this organism under suitable nutritional and physicochemical conditions resulted in high protein and lipid content in the biomass which depicted its suitability towards multiproduct paradigm. To that end, a biorefinery approach was adopted for CT02 biomass in two sequential steps, resulting in alternate product cascades of bioactive molecules and biodiesel or biofertilizer. At the onset, bioprospecting with different solvent-based crude extracts of CT02 biomass resulted in staggeringly high antioxidant

activity (IC_{50} value of 137 $\mu g\ mL^{-1}$ for acetone extract) and anticancer activity (IC_{50} value of 306.67 $\mu g\ mL^{-1}$ for ethyl acetate extract). In the next step, post extracted residual biomass of CT02 yielded high FAME content of 33.1–36.7% w/w. Analysis of FAME composition revealed abundance of palmitic acid (C16:0), stearic acid (C18:0), and elaidic acid (C18:1n9t) as the major constituents, proving it suitable for use as biodiesel. When purposed as biofertilizer, the post extracted residual biomass showed significant inductive effect on germination of *Solanum lycopersicum* seeds, comparable to that of commercial grade NPK. In a nutshell, sequential demonstration of CT02 as a cell factory for production of high value bioactive molecules and low value biodiesel or biofertilizer designated the strain to be a potential candidate for construction of biorefinery. Furthermore, commercial viability of the process can be enhanced by implantation of process engineering strategies at the cultivation of CT02 aiming high biomass titer and productivity.

Author contribution Ankan Sinha: Planning and execution of experiments, analysis and interpretation of data, and manuscript preparation. Gargi Goswami: Conceptualization and manuscript writing. Ratan Kumar: Experimentation and manuscript preparation. Debasish Das: Conceptualization, overall supervision of the work, and manuscript writing.

Availability of data All data generated or analyzed during this study are included in this article and its supplementary material.

Declarations

Conflict of interest The authors declare no competing interests.

References

1. Santos FM, Gonçalves AL, Pires JCM (2019) Negative emission technologies. Bioenergy with Carbon Capture Storage Using Nat Resour Sustain Dev 1–13. https://doi.org/10.1016/B978-0-12-816229-3.00001-6

2. Ferreira A, Ribeiro B, Ferreira AF et al (2019) Scenedesmus obliquus microalga-based biorefinery – from brewery effluent to bioactive compounds, biofuels and biofertilizers – aiming at a circular bioeconomy. Biofuels Bioprod Biorefin 13:1169–1186. https://doi.org/10.1002/bbb.2032

3. Nobre BP, Villalobos F, Barragán BE et al (2013) A biorefinery from Nannochloropsis sp. microalga - extraction of oils and pigments. Production of biohydrogen from the leftover biomass. Bioresour Technol 135:128–136. https://doi.org/10.1016/j.biortech.2012.11.084

4. Kothari R, Pandey A, Ahmad S et al (2017) Microalgal cultivation for value-added products: a critical enviro-economical assessment. 3 Biotech 7:1–15. https://doi.org/10.1007/s13205-017-0812-8

5. Muthuraj M, Kumar V, Palabhanvi B, Das D (2014) Evaluation of indigenous microalgal isolate Chlorella sp. FC2 IITG as a cell factory for biodiesel production and scale up in outdoor conditions. J Ind Microbiol Biotechnol 41:499–511. https://doi.org/10.1007/s10295-013-1397-9

6. Sen S, De B, Devanna N, Chakraborty R (2013) Total phenolic, total flavonoid content, and antioxidant capacity of the leaves of Meyna spinosa Roxb., an Indian medicinal plant. Chin J Nat Med 11:149–157. https://doi.org/10.1016/S1875-5364(13)60042-4

7. Pal U, Ghosh S (2020) Limaye AM (2020) DNA methylation in the upstream CpG island of the GPER locus and its relationship with GPER expression in colon cancer cell lines. Mol Biol Reports 4710(47):7547–7555. https://doi.org/10.1007/S11033-020-05817-5

8. Feng W, Zhu Y, Wu F et al (2015) (2015) Characterization of phosphorus forms in lake macrophytes and algae by solution 31P nuclear magnetic resonance spectroscopy. Environ Sci Pollut Res 238(23):7288–7297. https://doi.org/10.1007/S11356-015-5913-5

9. Parsons TR, Maita Y, Lalli CM et al (1984) Determination of phosphate. A Man Chem Biol Methods Seawater Anal 22–25. https://doi.org/10.1016/B978-0-08-030287-4.50015-3

10. Jain MS, Jambhulkar R, Kalamdhad AS (2018) Biochar amendment for batch composting of nitrogen rich organic waste: effect on degradation kinetics, composting physics and nutritional properties. Bioresour Technol 253:204–213. https://doi.org/10.1016/J.BIORTECH.2018.01.038

11. Cataldo DA, Haroon MH, Schrader LE, Youngs VL (1975) Rapid colorimetric determination of nitrate in plant tissue by nitration of salicylic acid. Commun Soil Sci Plant Anal 6:71–80. https://doi.org/10.1080/00103627509366547

12. Bradford MM (1976) A rapid and sensitive method for the quantitation of microgram quantities of protein utilizing the principle of protein-dye binding. Anal Biochem 72:248–254. https://doi.org/10.1016/0003-2697(76)90527-3

13. Strickland JDH, Parsons TR (1968) A practical handbook of sea water analysis. Bull Fish Res Board Can (Ottawa) 167:311

14. Bligh EG, Dyer WJ (1959) A rapid method of total lipid extraction and purification. Can J Biochem Physiol 37:911–917. https://doi.org/10.1139/O59-099

15. Dubois M, Gilles KA, Hamilton JK et al (1956) Colorimetric method for determination of sugars and related substances. Anal Chem 28:350–356. https://doi.org/10.1021/ac60111a017

16. Bhola V, Swalaha F, Ranjith Kumar R et al (2014) Overview of the potential of microalgae for CO2 sequestration. Int J Environ Sci Technol 11:2103–2118. https://doi.org/10.1007/s13762-013-0487-6

17. Solovchenko A, Khozin-Goldberg I (2013) High-CO2 tolerance in microalgae: possible mechanisms and implications for biotechnology and bioremediation. Biotechnol Lett 35:1745–1752. https://doi.org/10.1007/s10529-013-1274-7

18. Uggetti E, Sialve B, Hamelin J, et al (2018) CO2 addition to increase biomass production and control microalgae species in high rate algal ponds treating wastewater. J CO2 Util 28:292–298. https://doi.org/10.1016/j.jcou.2018.10.009

19. Wang H, Nche-Fambo FA, Yu Z, Chen F (2018) Using microalgal communities for high CO2-tolerant strain selection. Algal Res 35:253–261. https://doi.org/10.1016/j.algal.2018.08.038

20. Ren H-Y, Liu B-F, Ma C, et al (2013) A new lipid-rich microalga Scenedesmus sp. strain R-16 isolated using Nile red staining: effects of carbon and nitrogen sources and initial pH on the biomass and lipid production. Biotechnol Biofuels 61 6:1–10. https://doi.org/10.1186/1754-6834-6-143

21. Xin L, Hong-ying H, Ke G, Jia Y (2010) Growth and nutrient removal properties of a freshwater microalga Scenedesmus sp. LX1 under different kinds of nitrogen sources. Ecol Eng 36:379–381. https://doi.org/10.1016/j.ecoleng.2009.11.003

22. Wu YH, Yu Y, Hu HY, Zhuang LL (2016) Effects of cultivation conditions on the production of soluble algal products (SAPs) of Scenedesmus sp. LX1. Algal Res 16:376–382. https://doi.org/10.1016/j.algal.2016.04.006

23. Arumugam M, Agarwal A, Arya MC, Ahmed Z (2013) Influence of nitrogen sources on biomass productivity of microalgae Scenedesmus bijugatus. Bioresour Technol 131:246–249. https://doi.org/10.1016/j.biortech.2012.12.159

24. Shen Y, Yuan W, Pei Z, Mao E (2010) Heterotrophic culture of Chlorella protothecoides in various nitrogen sources for lipid production. Appl Biochem Biotechnol 160:1674–1684. https://doi.org/10.1007/s12010-009-8659-z

25. Goswami G, Sinha A, Kumar R, Dutta BC, Singh H, Das D (2019) Process engineering strategy for cultivation of high density microalgal biomass with improved productivity as a feedstock for production of bio-crude oil via hydrothermal liquefaction. Energy 189:116–136. https://doi.org/10.1016/j.energy.2019.116136

26. Muthuraj M, Chandra N, Palabhanvi B, Kumar V, Das D (2015) Process engineering for high-cell-density cultivation of lipid rich microalgal biomass of Chlorella sp FC2 IITG. Bioenergy Res 8(2):726–739. https://doi.org/10.1007/s12155-014-9552-3

27. Palabhanvi B, Muthuraj M, Mukherjee M, Kumar V, Das D (2016) Process engineering strategy for high cell density-lipid rich cultivation of Chlorella sp. FC2 IITG via model guided feeding recipe

and substrate driven pH control. Algal Res 16:317–329. https://doi.org/10.1016/j.algal.2016.03.024

28. Surkatti R, Al-Zuhair S (2018) Effect of cresols treatment by microalgae on the cells' composition. J Water Process Eng 26:250–256. https://doi.org/10.1016/j.jwpe.2018.10.022

29. Sánchez Mirón A, Cerón García MC, García Camacho F et al (2002) Growth and biochemical characterization of microalgal biomass produced in bubble column and airlift photobioreactors: studies in fed-batch culture. Enzyme Microb Technol 31:1015–1023. https://doi.org/10.1016/S0141-0229(02)00229-6

30. Wang L, Wang L, Manzi HP et al (2020) Isolation and screening of Tetradesmus dimorphus and Desmodesmus asymmetricus from natural habitats in Northwestern China for clean fuel production and N, P removal. Biomass Convers Biorefinery. https://doi.org/10.1007/s13399-020-01034-z

31. Mishra S, Mohanty K (2019) Comprehensive characterization of microalgal isolates and lipid-extracted biomass as zero-waste bioenergy feedstock: an integrated bioremediation and biorefinery approach. Bioresour Technol 273:177–184. https://doi.org/10.1016/j.biortech.2018.11.012

32. Banskota AH, Sperker S, Stefanova R et al (2019) Antioxidant properties and lipid composition of selected microalgae. J Appl Phycol 31:309–318. https://doi.org/10.1007/s10811-018-1523-1

33. Lourenço SC, Moldão-Martins M, Alves VD (2019) Antioxidants of natural plant origins: from sources to food industry applications. Molecules 24:14–16. https://doi.org/10.3390/molecules24224132

34. Sathisha AD, Lingaraju HB, Prasad KS (2011) Evaluation of antioxidant activity of medicinal plant extracts produced for commercial purpose. E-Journal Chem 8:882–886. https://doi.org/10.1155/2011/693417

35. Dimova D, Dobreva D, Panayotova V, Makedonski L (2021) DPPH antiradical activity and total phenolic content of methanol and ethanol extracts from macroalgae (Ulva rigida) and microalgae (Chlorella). Scr Sci Pharm 6:37. https://doi.org/10.14748/ssp.v7i2.7369

36. Cengiz Sahin S (2019) Scenedesmus obliquus: a potential natural source for cosmetic industry. Int J Second Metab 6:129–136. https://doi.org/10.21448/ijsm.545771

37. Assunção MFG, Amaral R, Martins CB et al (2017) Screening microalgae as potential sources of antioxidants. J Appl Phycol 29:865–877. https://doi.org/10.1007/s10811-016-0980-7

38. Ambi A, Bauchi FP, Bashir M (2021) Yellow and red varieties of Hibiscus sabdariffa calyces contain novel antioxidants as analysed by liquid chromatography-electrospray ionization tandem mass spectrometry (LC-ESI) Acta Scientific NUTRITIONAL HEALTH (ISSN : 2582–1423) Yellow and Red Varie

39. Mène-Saffrané L, Jones AD, DellaPenna D (2010) Plastochromanol-8 and tocopherols are essential lipid-soluble antioxidants during seed desiccation and quiescence in Arabidopsis. Proc Natl Acad Sci U S A 107:17815–17820. https://doi.org/10.1073/pnas.1006971107

40. Kim BR, Kim HM, Jin CH et al (2020) Composition and antioxidant activities of volatile organic compounds in radiation-bred coreopsis cultivars. Plants 9. https://doi.org/10.3390/plants9060717

41. Jamil MDHM, Taher M, Susanti D et al (2020) Phytochemistry, traditional use and pharmacological activity of Picrasma quassioides: a critical reviews. Nutrition 12:2584. https://doi.org/10.3390/NU12092584

42. Dubuisson M, Marchand C, Rees JF (2004) Firefly luciferin as antioxidant and light emitter: the evolution of insect bioluminescence. Luminescence 19:339–344. https://doi.org/10.1002/bio.789

43. Salehi B, Azzini E, Zucca P et al (2020) Plant-derived bioactives and oxidative stress-related disorders: a key trend towards healthy aging and longevity promotion. Appl Sci 10. https://doi.org/10.3390/app10030947

44. Puente-Garza CA, Meza-Miranda C, Ochoa-Martínez D, García-Lara S (2017) Effect of in vitro drought stress on phenolic acids, flavonols, saponins, and antioxidant activity in Agave salmiana. Plant Physiol Biochem 115:400–407. https://doi.org/10.1016/j.plaphy.2017.04.012

45. Bajguz A (2010) An enhancing effect of exogenous brassinolide on the growth and antioxidant activity in Chlorella vulgaris cultures under heavy metals stress. Environ Exp Bot 68:175–179. https://doi.org/10.1016/j.envexpbot.2009.11.003

46. Dawood Shah M, Seelan Sathiya Seelan J, Iqbal M (2020) Phytochemical investigation and antioxidant activities of methanol extract, methanol fractions and essential oil of Dillenia suffruticosa leaves. Arab J Chem 13:7170–7182. https://doi.org/10.1016/j.arabjc.2020.07.022

47. Shah MD, Yong YS, Iqbal M (2014) Phytochemical investigation and free radical scavenging activities of essential oil, methanol extract and methanol fractions of Nephrolepis biserrata. Int J Pharm Pharm Sci 6:269–277

48. Aumsuwan P, Khan SI, Khan IA et al (2016) The anticancer potential of steroidal saponin, dioscin, isolated from wild yam (Dioscorea villosa) root extract in invasive human breast cancer cell line MDA-MB-231 in vitro. Arch Biochem Biophys 591:98–110. https://doi.org/10.1016/j.abb.2015.12.001

49. Agarwal DS, Anantaraju HS, Sriram D et al (2016) Synthesis, characterization and biological evaluation of bile acid-aromatic/heteroaromatic amides linked via amino acids as anti-cancer agents. Steroids 107:87–97. https://doi.org/10.1016/j.steroids.2015.12.022

50. Kaskova ZM, Tsarkova AS, Yampolsky IV (2016) 1001 lights: Luciferins, luciferases, their mechanisms of action and applications in chemical analysis, biology and medicine. Chem Soc Rev 45:6048–6077. https://doi.org/10.1039/c6cs00296j

51. Min HY, Jang HJ, Park KH et al (2019) The natural compound gracillin exerts potent antitumor activity by targeting mitochondrial complex II. Cell Death Dis 10. https://doi.org/10.1038/s41419-019-2041-z

52. Kang HM, Son HS, Cui YH, et al (2017) Phytosphingosine exhibits an anti-epithelial-mesenchymal transition function by the inhibition of EGFR signaling in human breast cancer cells. Oncotarget 8:77794–77808. https://doi.org/10.18632/oncotarget.20783

53. Mahdavian E, Palyok P, Adelmund S et al (2014) Biological activities of fusarochromanone: a potent anti-cancer agent. BMC Res Notes 7:1–11. https://doi.org/10.1186/1756-0500-7-601

54. Habila MM, Festus EA, Morumda D, Joseph I (2021) FTIR and GC-MS analysis of the aqueous and ethanolic extracts of Jatropha tanjorensis leaves

55. Han HS, Kwon YJ, Park SH et al (2004) Potent effect of 5-HPBR, a butanoate derivative of 4-HPR, on cell growth and apoptosis in cancer cells. Int J Cancer 109:58–64. https://doi.org/10.1002/ijc.11643

56. Aminzadeh-Gohari S, Feichtinger RG, Vidali S et al (2017) A ketogenic diet supplemented with medium-chain triglycerides enhances the anti-tumor and anti-angiogenic efficacy of chemotherapy on neuroblastoma xenografts in a CD1-nu mouse model. Oncotarget 8:64728–64744. https://doi.org/10.18632/oncotarget.20041

57. Marrez DA, Naguib MM, Sultan YY, Higazy AM (2019) Antimicrobial and anticancer activities of Scenedesmus obliquus metabolites. Heliyon 5:e01404. https://doi.org/10.1016/j.heliyon.2019.e01404

58. Reyna-Martinez R, Gomez-Flores R, López-Chuken U et al (2018) Antitumor activity of Chlorella sorokiniana and

Scenedesmus sp. microalgae native of Nuevo León State. México PeerJ 2018:1–15. https://doi.org/10.7717/peerj.4358

59. Tavares-Carreón F, De La Torre-Zavala S, Arocha-Garza HF et al (2020) In vitro anticancer activity of methanolic extract of Granulocystopsis sp., a microalgae from an oligotrophic oasis in the Chihuahuan desert. PeerJ 2020:1–21. https://doi.org/10.7717/peerj.8686

60. Cha TS, Chen JW, Goh EG et al (2011) Differential regulation of fatty acid biosynthesis in two Chlorella species in response to nitrate treatments and the potential of binary blending microalgae oils for biodiesel application. Bioresour Technol 102:10633–10640. https://doi.org/10.1016/j.biortech.2011.09.042

61. Singh N, Goyal A, Moholkar VS (2020) Microalgal bio-refinery approach for utilization of Tetradesmus obliquus biomass for biodiesel production. Mater Today Proc 32:760–763. https://doi.org/10.1016/j.matpr.2020.03.541

62. Kumar V, Muthuraj M, Palabhanvi B et al (2014) High cell density lipid rich cultivation of a novel microalgal isolate Chlorella sorokiniana FC6 IITG in a single-stage fed-batch mode under mixotrophic condition. Bioresour Technol 170:115–124. https://doi.org/10.1016/j.biortech.2014.07.066

63. Gouveia L, Oliveira AC (2009) Microalgae as a raw material for biofuels production. J Ind Microbiol Biotechnol 36:269–274. https://doi.org/10.1007/s10295-008-0495-6

64. Aslam A, Thomas-Hall SR, Manzoor M et al (2018) Mixed microalgae consortia growth under higher concentration of CO_2 from unfiltered coal fired flue gas: fatty acid profiling and biodiesel production. J Photochem Photobiol B Biol 179:126–133. https://doi.org/10.1016/j.jphotobiol.2018.01.003

65. Mukherjee C, Chowdhury R, Ray K (2015) Phosphorus recycling from an unexplored source by polyphosphate accumulating microalgae and cyanobacteria-a step to phosphorus security in agriculture. Front Microbiol 6:1–7. https://doi.org/10.3389/fmicb.2015.01421

66. Nayak M, Swain DK, Sen R (2019) Strategic valorization of de-oiled microalgal biomass waste as biofertilizer for sustainable and improved agriculture of rice (Oryza sativa L.) crop. Sci Total Environ 682:475–484. https://doi.org/10.1016/j.scitotenv.2019.05.123